

AEROELASTICITY OF VERY HIGH L/D BODIES IN SUPERSONIC FLIGHT: NUMERICAL AND EXPERIMENTAL RESULTS

S. Heddadj¹, R. Cayzac¹, J. Renard² and M. Giraud³

¹ *Giat Industries, Division des Systèmes d'Armes et de Munitions, 7 route de Guerry,
18023 Bourges Cedex, France*

² *Université d'Orléans, Laboratoire Energétique-Explosions-Structures,
63 Avenue de Lattre de Tassigny, 18020 Bourges, France*

³ *ISL, French-German Research Institute, BP 34, F-68301 Saint-Louis, France*

The complete equations of motion of a flexible supersonic high L/D body are presented. The bending is represented by cutting the projectile into two parts, both of which behave like rigid bodies. A Lagrangian approach is used which leads to a linear set of equations, which are numerically solved, in order to analyze the system stability. A parametric study is then presented, to evaluate the influence of chosen parameters (initial conditions, body rigidity, steady state roll rate) on this stability. These numerical results are then compared with small scale firing tests results, thus leading to a qualitative validation of the model and its mathematical formulation.

INTRODUCTION

The in-flight behavior of high L/D ratio projectiles may present detrimental aeroelastic effects, because of the destabilizing feature of the flow-oscillating mechanical structure coupling. The problem specificity, relative to normal practice in the aeronautic field, is the result of the very high constraints and accelerations the body undergoes during the launch, the particular geometric configuration of the latter and the very high speeds considered, as well as the roll movement. This study is aimed at highlighting the influence of aeroelasticity on firing accuracy and dispersion. It includes the construction of a numerical model with an adequate formulation of the motion equations and firing tests for validation purposes. It is carried out in association with the ISL (French-German Research Institute) and with the University of Orleans.

NUMERICAL APPROACH

Model Presentation [1]

The bending is represented by “cutting” the body into two parts (see Fig. 1), connected by what we’ll call an “elastic ball joint”. This type of joint allows the same degrees of freedom as a ball joint (three rotational degrees) but is able to transmit torques. We then have a body in two parts, both of which behave like rigid bodies and are connected at one point, named A.

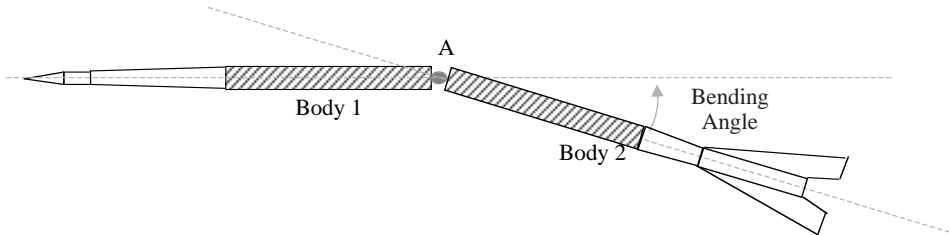


Figure 1: Mechanical model.

The rear part has three degrees of freedom relative to the fore part (two degrees of flexion in the pitch and yaw directions and one degree of torsion in the longitudinal direction). We thus have a nine degree of freedom system: three translational degrees for the connecting point and three rotational degrees for each body.

This simplified model was chosen, as a first approximation, for many reasons:

- the first reason stems from a bibliographic study and is the result according to which only the first bending mode has a significant influence on the body stability [2],
- this representation enables a partition of the aerodynamic load,
- the problem can be treated by rigid-body dynamics, as each body behaves mechanically like a rigid body. If necessary, it is then possible to write the equations of motion, while taking large displacements into account (non linear equations),
- lastly, this first approach allows an extension towards the study of a continuous system. Actually, it is possible for three, four, ... n bodies to be considered later on.

Equations of Motion

A Lagrangian approach was used in order to write the equations of motion of the model. The nine Lagrangian equations were firstly written and linearized. The aerodynamic load was determined and linearized in terms of the generalized coordinates. The system could then be written in a matrix form.

Lagrange's equations are given by:

$$\frac{d}{dt} \left(\frac{\partial T}{\partial \dot{q}_j} \right) - \frac{\partial T}{\partial q_j} = \Pi_j \quad (1)$$

where q_j represent the independent generalized coordinates, T is the kinetic energy of the whole body and Π_j are the generalized forces ($j = 1$ to 9).

We have nine independent generalized coordinates that correspond to the nine degrees of freedom (DOF). We then have six angles, corresponding to the three rotational DOF of each of the two bodies, and the three coordinates of point A. The equations are written in a particular coordinate frame, that enables linearization, that is to say a coordinate frame where generalized coordinates are small quantities. This coordinate frame actually represents the "ideal" position and trajectory of the body. It has a translatory movement (relative to the earth) at speed u , where u is the velocity of the body and a rotational movement, representing the roll movement. The generalized coordinates are expressed in that coordinate frame and then represent the small displacements of the body relative to its "ideal" configuration.

The calculation of the generalized forces implies the aerodynamic load evaluation. In order to determine the aerodynamic forces applied to the two bodies, we make a stationary assumption: the load is evaluated for different flexed configurations of the body, without taking the flexing oscillations into account. This can be justified by comparing the characteristic time of the flow with the characteristic time of flexing (ratio about 15). The aerodynamic forces and moments are calculated, firstly using the SHABP code [3] (Supersonic Hypersonic Arbitrary Body Program). Later, CFD calculations using FLU3M code [4] (Euler and Navier Stokes equations) will be considered.

The SHABP code does not calculate the Magnus force, nor the Magnus moment coefficients. Neither does it provide the damping moment coefficients (roll, pitch, yaw). These coefficients are, as a first approximation, considered constant and equal to the rigid body values (obtained from wind tunnel tests [5]).

Aerodynamics coefficients are found, that are either constants, or linear in terms of generalized coordinates. We then obtain a linear set of equations, which can be written as follows:

$$[M] \ddot{X} + ([G] + [C]) \dot{X} + [K^*] X = F_0 \quad (2)$$

where $[M]$ is a mass matrix, $[G]$ is a gyroscopic matrix, $[C]$ is a damping matrix and $[K^*]$ is a stiffness matrix modified by centrifugal and aerodynamic forces.

Numerical Resolution

With no roll and no aerodynamic load, the system of equations has 4 zero natural frequencies, that correspond to rigid body modes and a double frequency that corresponds to the first static bending frequency. With a non zero roll rate and an aerodynamic load, the frequencies become complex quantities and we will focus our attention on the real part, which indicates the stability of the projectile. Indeed, when the real part of one of the frequencies becomes positive, it corresponds to an exponential amplification of perturba-

tions. The advantage of the natural frequencies study is that it enables rapid prediction of key parameters (roll rate, rigidity, ...). The drawback is that the velocity of the projectile and its roll rate are considered constant and gravity can't be taken into account. That's why an implicit resolution of the motion equations has also been carried out.

The aim of the resolution program is to know, at any instant of the flight, the position and orientation of the body, that is to say the coordinates of point A (see Fig. 1), the angle of attack and the flexure angle of the body. A Newmark [6] method (corresponding to an implicit formulation) is used. This method is a one-step time dependent integration method. The system state at a given time $t_{n+1} = t_n + h$ is evaluated from the known state at time t_n thanks to Taylor's formula. The results obtained are then compared with those obtained with a rigid body 6-Degrees-Of-Freedom code. We then impose a high rigidity (10000 times bigger than the real value) in our formulation to be under the same conditions. This enabled program validation in the rigid body case.

The first result is that bending may be created by aerodynamics, even when no initial flexure is induced during the launch. Yet this bending is of low intensity.

When assuming an initial flexure of the body, the phenomenon is rapidly damped if the initial angles of attack of the fore and rear parts of the body are of different signs. If this is not the case, the natural frequencies excited are not the same and the damping is much lower.

The most influential parameter seems to be the steady state roll rate, as it has an influence on the frequencies excited, but also on the aerodynamic load. Increasing its value leads to an amplification of the destabilizing patterns (bending angle and angle of attack for example). We can then highlight a critical roll rate, above which we have instability. Yet, this critical roll rate also exists for the rigid body and is linked to the Magnus effects. But what we can note is that its value depends on the projectile flexibility. The more rigid the projectile, the higher the critical roll rate

To obtain validation of these first numerical results, experiments have been carried out.

EXPERIMENTAL APPROACH

Experimental Device

A whole series of small scale firing tests have been carried out in the 100 meter free flight ballistics corridor at ISL, using a 30 mm gun. Smooth projectiles, with an L/D ratio of up to 70 (to enhance the bending phenomenon) have been fired at Mach 3. Projectiles, with a three-component sabot, are pushed during the launch. Many of these firings were aimed at determining the conditions (body geometry, launch) under which the bending phenomenon was significant but not so much so that it strongly modified the trajectory. It was then possible to vary different parameters such as the roll rate for instance.

Aeroelastic free flight behaviour of the projectile is investigated by use of a multiple orthogonal shadow visualisation technique (8 double shadowgraphic stations, in the vertical and horizontal planes) and of the yaw card technique. The speed of the projectile is measured by use of a Doppler radar.

Exploitation and First Comparative Results

For each shadowgraph, points along the curved cylindrical part of the projectile are recorded (plus two points characterizing the firing axis). We thus have the spatial coordinates of the bent rod at our disposal and this is very rich in information.

First, it enables the plane in which the bending occurs to be determined. Indeed, it was verified, on all photographs of many firings, that bending is planar, that is to say there is no torsion. It is then possible for the new coordinates of the points along the bent rod to be written in the bending plane, so as to obtain the real bending aspect. We can then verify if this aspect is close to the first bending mode or not, which would justify the chosen model. Fig. 2 presents the results obtained for 3 successive shadowgraphs of a particular firing (chosen because the bending amplitude was one of the largest obtained). Squares represent values measured from shadowgraphs, whereas the continuous line represents the analytical first bending mode aspect of an equivalent free-free beam with a circular cross section.

For all analyzed photographs, the bending aspect was close to the first mode, especially when the bending amplitude is high. For a slightly bent rod, this is less true, maybe because in that case, the measurement relative error becomes more important.

In fact, the shadowgraphs give us the position, orientation and bending of the projectile at 8 successive times (about one millisecond between two shadowgraphs). It is sufficient to obtain at least two periods of bending oscillations, but there are few points in one period, which makes it difficult to interpolate from them (see Fig. 3, which represents the bending angle versus distance from the gun muzzle).

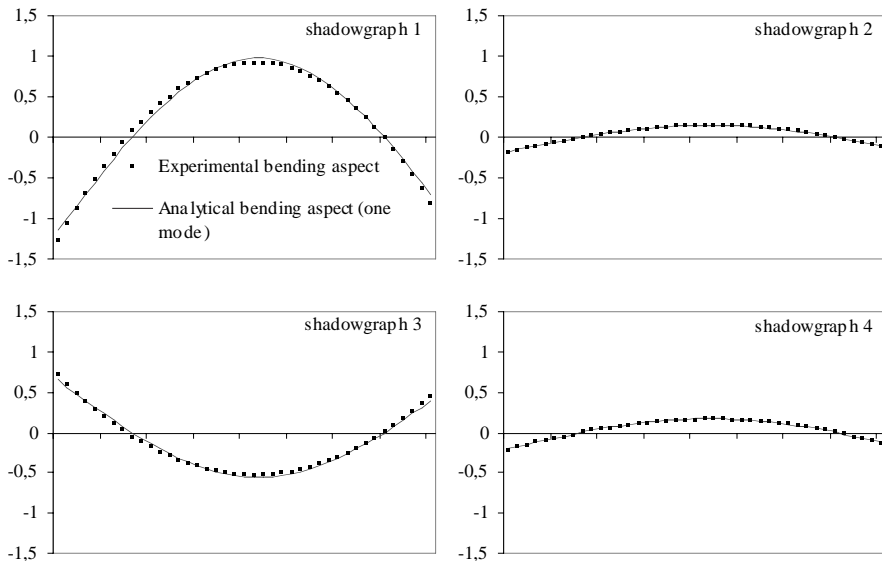


Figure 2: Comparisons experimental / analytical first mode bending aspect.

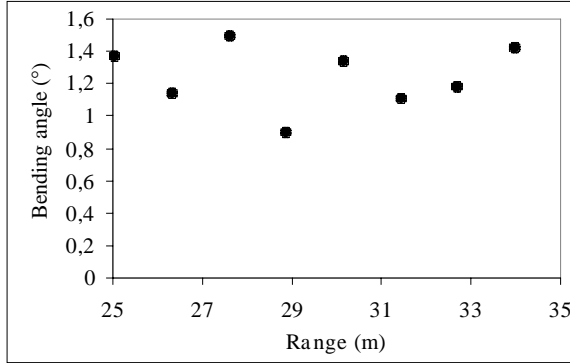


Figure 3: Experimental bending angle.

We then analyse yaw cards. For a rigid body, yaw card study can provide the following quantities: the roll angle ϕ , the precession ψ (orientation of the resistance plane respect to the vertical plane containing the velocity vector), the angle of attack d . In our case, the imprint in the yaw card is the result of combined orientation and bending of the body. We thus defined effective quantities ϕ_{eff} , ψ_{eff} , δ_{eff} , corresponding to the equivalent imprint of a rigid body.

First, we compared yaw card results with shadowgraph results. Fig. 6 represents δ_{eff} versus distance from the gun muzzle. Square symbols are obtained from yaw cards and circle symbols from shadowgraphs.

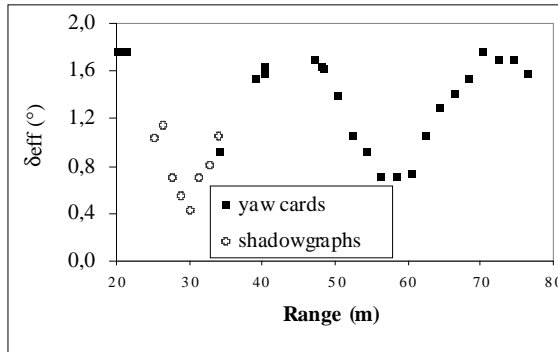


Figure 4: Correlation between yaw cards / shadowgraphs results.

Comparison is satisfactory and we can note that the curves seem perturbed, as compared with curves obtained with a rigid body. In the same way, Fig. 5 shows the same sort of perturbations on the Angle of attack/Precession (delta/psi) polar diagram. The theoretical rigid body curve is represented by the dotted line, experimental values by the crosses and the theoretical flexible body curve by the continuous line (for an initial 2 degree bending angle).

This is not due to measurement inaccuracy, but to the body bending. This qualitatively substantiates the numerical results, which enhance the influence of bending on the trajec-

tory parameters. Fig 6 and 7 show that a higher frequency superimposes the main frequency and corresponds to the bending frequency.

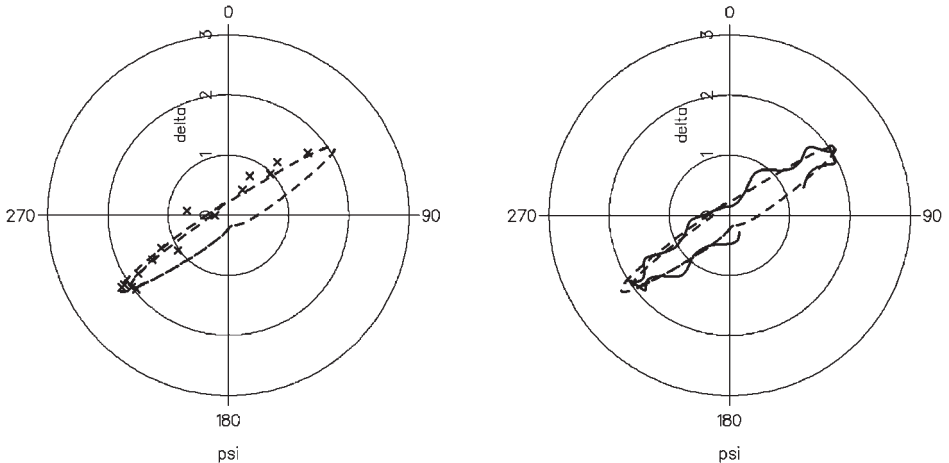


Figure 5: Comparison numerical / experimental polar diagram.

CONCLUSION AND PERSPECTIVES

A complete linear set of equations, describing the motion and bending of a supersonic high L/D body was written, using a Lagrangian formulation. A study of the first natural frequencies and a program of resolution of these equations was then carried out, leading to an evaluation of the influence of key parameters on the projectile's dynamic behavior. The parameter that influences stability most seems to be the roll rate, which has an influence on the natural frequencies excited and also on the aerodynamic load.

Firings test have been carried out and provided purely experimental results. For example, for all firings considered, bending was planar and the bending aspect was close to the first mode aspect. Moreover, these experiments have also qualitatively substantiated numerical results.

Many ways are considered to improve this study. The first one is a resolution of the complete coupled system (no linearization). It is also possible to consider more than two rigid parts for bending representation. Lastly, the aerodynamic load evaluation can be improved, by use of CFD calculations.

REFERENCES

1. Heddadj, S., Cayzac, R., Renard, J., "Aeroelasticity of supersonic high L/D bodies: Theoretical and numerical approach", *AIAA paper no 2000-0390*, 38th Aerospace Sciences Meeting and Exhibit, Reno, Jan. 2000
2. Platus, D.H., "Aeroelastic stability of Slender, Spinning Missiles", *Journal of Guidance, Control, and Dynamics*, Vol. 15, No 1, 1992, pp.144-151
3. Lecuyer M., "Prévision des Coefficients Aérodynamiques de Véhicules Hypersoniques par les Codes HABP et SHABP. Comparaisons avec l'Expérience", *Conférence AAAF*, Poitiers, 1987
4. Guillen P. and Dormieux M., "Design of a 3D Multidomain Euler Code", *Proceedings of the International Seminar on Supercomputing in Fluid Flow*, Boston, USA, 1989.
5. Rapport d'essais Obus flèche de 120 mm. Mesure en soufflerie des coefficients aerodynamiques No 29/93/SAE/E51/RE29/CI.
6. Gérardin, M. and Rixen, D., "Théorie des vibrations", Masson, 1992